

METER-SCALE OBSERVATIONS OF AIRCRAFT WAKE VORTICES IN PRECIPITATION USING A HIGH RESOLUTION SOLID-STATE W-BAND RADAR

THOMAS A. SELIGA^{1*} AND JAMES B. MEAD²

1. USDOT NATIONAL TRANSPORTATION SYSTEMS CENTER, CAMBRIDGE, MASSACHUSETTS
2. PROSENSING, INC., AMHERST, MASSACHUSETTS

1. INTRODUCTION*

Detection, tracking and characterization of wake vortices generated by aircraft during takeoff and landing are important to assess threats to aviation safety and ensuring that air traffic control procedures adequately account for the phenomenon [cf. Hallock et al., 1998; Gerz et al. (2001, 2002), Mackey et al. (2007), FAA(2008), Wassaf et al. (2008)]. The issue has attracted international attention over many decades as demonstrated, for example, by related activities of the aviation community that include the Federal Aviation Administration (FAA) and NASA in the United States (Broderick et al., 2008) and the European Commission (WakeNet, est. 1998).

This paper reports on a radar technology that may provide valuable contributions to these efforts. Specifically, meter-scale detection of aircraft wake vortices in light rain has been demonstrated using a low power (100-mW), solid-state W-Band (94-GHz) radar system. The radar employs a 1.2 m diameter antenna on a scanning pedestal, providing a 1.5-m 6-dB cross-track beam pattern at 500-m range. Range resolution as fine as 1.0-m is achieved using stretch processing, which also provides processing gain on the order of 30 dB. Additional coherent gain is achieved through FFT processing at each range gate. Range sidelobe suppression of greater than 40-dB makes this system suitable for high spatial and temporal resolution meteorological research such as the investigation of wake turbulence behavior during aircraft takeoff and landing operations.

Aircraft wake vortex measurements in light rain were gathered in the spring of 2009 at Logan International Airport at a range of 480-1,050-m. Spectral data in the absence of wake vortices exhibit very narrow spectral widths (on the order of 10-20 $\text{cm}\cdot\text{s}^{-1}$); this is attributed to the lack of shear within the small resolution volume. Classic counter rotating vortices were observed when making RHI scans perpendicular to the aircraft flight vector. Reflectivity RHI plots showed clear evidence of enhanced droplet concentration between the vortices, with a dramatic reduction in droplet concentration in columns directly below and towards the outside of each vortex. These structures in reflectivity were observed to persist for approximately 60 seconds after passage of the aircraft, consistent with the typical lifetime of vortices generated by landing aircraft.

The W-band radar was deployed in March 2009 as part of the Tall Vessel Detection System (TVDS) at Logan International Airport. Its primary function is to measure the height of marine vessels in Boston Harbor. The W-

band radar's design parameters are seen to relate very well to investigations of basic meteorological phenomena as well, particularly at the microscale, which includes wake turbulence and many features of boundary layer meteorology.

2. RADAR UTILITY AND DESIGN

The arrival and departure zone of the primary runway of Boston's Logan International Airport resides within a major portion of Boston Harbor; this region of the Harbor is considered the Runway Protection Zone (RPZ). Since the Harbor is often inhabited by tall marine vessels of various types and heights, air traffic controllers are required to account for the presence of such vessels within this zone when managing air traffic operations on this runway. The 94-GHz radar, discussed here, was designed as part of a dual-radar system for detecting, tracking and measuring the height of vessels transiting the Harbor (Mead et al., 2009). The radar is essentially programmed to act as a search-light sensor that measures the heights of tall vessels, which are then indicated on a display of the Harbor in the Air Traffic Control Tower.

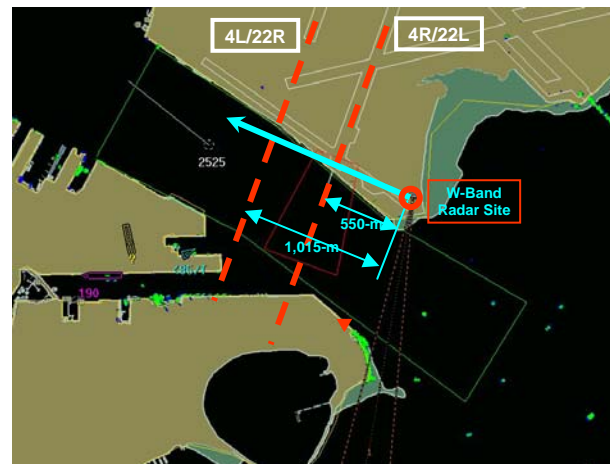


Fig. 1. Location of the W-Band Radar at Boston's Logan International Airport. Centerlines for Runways 4R/22L and 4L/22R are shown as dashed red lines. The red-filled triangle signifies the location of the reference trihedral reflector used for calibration of the system.

2.1 Design Attributes

The W-Band Radar and antenna are contained in a secure shelter, located on the airfield where it is able to scan designated surveillance zones of the Harbor as shown in Fig. 1. The figure also shows that the location is very well situated by orientation and distance from Runways 4R/22L and 4L/22R to perform RHI scans in a

* Corresponding author address: Thomas A. Seliga, Volpe National Transportation Systems Center, 55 Broadway, Cambridge, MA 02142, e-mail: Thomas.Seliga@dot.gov

plane normal to the landing flight path of aircraft landing on or taking off from these parallel runways. This scanning configuration is preferred for the remote sensing of wake vortices being shed from aircraft that are landing and taking off. Another feature of the radar system is a trihedral reference reflector that is located across the Harbor from the airfield at a distance of approximately 1-km from the radar. The reflector provides for regular sampling of a known, high intensity reference radar cross section signal that is used to monitor functionality and calibrate the radar during attenuation events such as fog and rainfall.



Fig. 2. Photograph of the W-Band Radar Shelter at Logan International Airport, showing the Boston skyline. The antenna (see Fig. 4) is housed in the cylindrically-shaped radome on the left.



Fig. 3. W-Band Radar Antenna and Pedestal.

The radar shelter was specially designed for the marine vessel height detection application and is shown in Fig. 2. The antenna is a parabolic Cassegrain-feed reflector located on one end of the shelter as shown in Fig. 3. The nominal antenna gain is 58-dB, and its half-power beamwidth is 0.18° as indicated in the pattern measured by the manufacturer in Fig. 4. The radar operates at vertical polarization. The classical near-field Fresnel region extends out to a range of ~ 625 -m, but the radiation beam is known to be well-formed or near Gaussian much nearer to the antenna, indicating that reliable radar measurements are possible starting at ranges of ~ 300 -m. Thus, the cross-range resolution of

the radar at the distances of interest for wake vortex measurements at Logan Airport range between approximately 1- to 5-m at ranges from 300- to 1,500-m, respectively. The shelter limits the maximum elevation angle of the antenna to 15° .

A simplified block diagram of the radar is shown in Fig. 5 with specifications listed in Table 1. The radar incorporates a stretch processor, transmitting a long-duration, linear FM chirp waveform. The duration of the signal is configurable from 1-10- μ s. The received signal is multiplied by a time-delayed receiver local oscillator waveform of the same slope in the modulation domain (frequency vs. time) used for transmission. The resultant waveform is sampled at 200 -MHz- s^{-1} and then processed by a first level FFT to generate a range profile with meter-scale range resolution. The radar operates at a 20-kHz pulse repetition frequency, yielding an unambiguous Doppler interval of ± 16 -m- s^{-1} and allowing for a large number of samples to be coherently integrated to improve sensitivity. The typical coherent integration length is 256 samples, implemented by a second level FFT at each range gate that performs the Doppler processing. This sampling length produces a Doppler velocity resolution of ~ 0.12 -m- s^{-1} . The integration length can also be increased to 512 or 1,024 samples, depending on the application, increasing the resolution by factors of 2 or 4, respectively. The resultant velocity spectra are power-averaged to reduce fading and then sent on to an analysis program to implement clutter filtering for the marine vessel height measurement application.

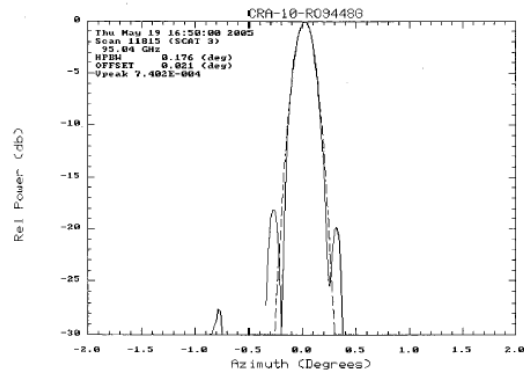


Fig. 4. Sample W-Band Radar antenna radiation pattern as measured by the manufacturer, Millitech Corporation.

Several other features of the radar are worth mentioning. While numerically intensive signal processing functions are implemented in C, the algorithms used to schedule radar scanning, implement CFAR processing and estimate ship height are written in the IDL language. This approach allows for rapid code development and access to sophisticated graphical tools for data visualization. A single multi-core PC server is able to handle all radar control, signal processing and data analysis tasks. Internet connectivity to the radar server extends access of the radar to remote sites and enables rapid prototyping of additional radar processing schemes and products. The arrangement also provides for ready access to archived

data and the transfer of data to remote sites for further archiving and processing. Radar performance can be continuously monitored for maintenance and carefully scrutinized via access to several weeks of raw radar data that are archived at the radar site. Provisions for archiving of these data off site on a remote server, such as one located at ProSensing's facility in Amherst, MA, have also been implemented.

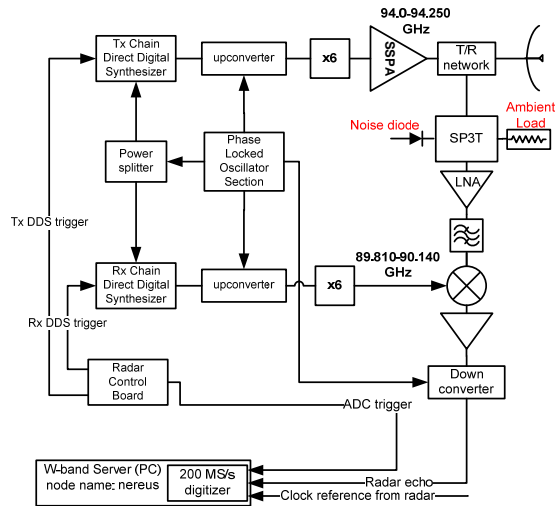


Fig. 5. Block Diagram of the W-Band Radar System.

Table 1. W-Band Radar Specifications.

Parameter	Value
Frequency of Operation	94.0-94.25 GHz
Peak Transmit Power	100 mW
Waveform Type	Linear FM chirp
Range Resolution	1.0 m
Pulse Repetition Frequency	20 kHz
Pulse Duration (min- max)	1-10 μ s
Antenna Diameter & Type	48" Cassegrain
Antenna Beamwidth	0.18 $^\circ$
Antenna Gain	58 dB
Front-end Noise Figure	12 dB

2.2 Performance Validation of Doppler Velocity

Since the topic of this paper deals with Doppler velocity measurements of wake vortices, this section presents data that demonstrate the validity of the radar measurements compared to wind speed measurements at the airport's ASOS site. On July 24, 2009, a long duration high wind event occurred at the airport with winds exceeding 20-kts in a direction nearly parallel to the line-of-sight between the radar and the reference reflector. The presence of light rain during much of the day made it possible to compare radar wind measurements derived from Doppler velocities with ASOS 1-min observations. An example of this comparison is presented here in order to validate the radar's Doppler velocity measurements.

Fig. 6 shows a video camera picture of the tower on which the reference reflector is mounted at a height of

~82-ft MSL; the picture was taken from the site of the W-Band Radar at 07:52:31 EDT. Fig. 7 is a corresponding W-Band Radar range-velocity profile with 256 sample FFT processing of the reference reflector and adjacent range gates between ranges of ~930- to 1,083-m at this same time. The strong reference signal at zero Doppler velocity is clearly seen at a range of ~1,013-m along with its associated range sidelobes that are typically suppressed by more than 40-dB at distances greater than ~5-m from the reflector. Doppler sidelobes are also evident in the figure, but these are suppressed by more than 50-dB over most of the Doppler spectral interval. The rain signature appears as a narrow dark-blue band between 8 and 12 m-s $^{-1}$. The average Doppler velocity over the measurement range swath of ~153-m was 10.7-m-s $^{-1}$. This compares with the two-minute average component of the ASOS winds of 8.6-m-s $^{-1}$ recorded at 17:53:00 EDT, a difference of 2.1-m-s $^{-1}$. This difference is readily attributable to the difference in the heights of the two measurements; the radar Doppler measurements were at ~82-ft while the ASOS were at ~45.8-ft MSL. It is reasonable to assume that the range of wind variation with height typically follows a power-law relationship given by

$$u_z = u_{10} \left(\frac{z}{z_{10}} \right)^\alpha \quad (1)$$

where u_h is the horizontal wind speed at height h , u_{10} is the wind speed at 10-m height, z is the height of interest AGL, z_{10} is 10-m AGL and α is the Hellman (1917) constant, ranging typically between around 0.1 to 0.3 near coastal areas such as Logan Airport. Based on this consideration, the height transformation of the ASOS wind speed in the direction and at the height of the radar Doppler measurements would be between 9.3- to 10.8-m-s $^{-1}$ in good agreement with the 10.7-m-s $^{-1}$ average Doppler velocity measurement at the height of the reference reflector. This comparison and many others (including measurements of hard targets such as ships and boats moving in different directions throughout the Boston Harbor surveillance zones), not shown here, validated the Doppler velocity measurement capabilities of the radar.



Fig. 6. Video camera view of the tower on which the trihedral reference reflector is mounted. The horizontal distance of the tower from the radar is 1.0-km. Note that in this case the meteorological optical range is in excess of 1-km.

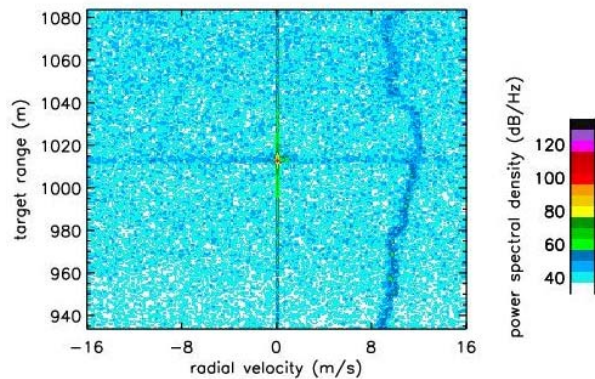


Fig. 7. Doppler velocity profile with range between ~930- to 1,083-m. The reference target is seen as the strong target with zero velocity, located at a range of ~1,013-m from the radar.

3. WAKE VORTEX DETECTION

In order for the W-Band Radar to detect wake vortices generated by aircraft, scatterers such as hydrometeors or chaff must be present in the scattering volume. The sensitivity of the W-Band Radar is estimated to be between around -15 to -10 dBZ at a range of 1-km. This sensitivity may also be further compromised by attenuation effects caused by fog and precipitation along the propagation path to the scattering volume. Although attenuation can be severe in the presence of liquid water (Ulaby et al., 1981), most precipitation events would readily accommodate the detection of wake vortices at distances less than 1- to 2-km with this radar.

Normal procedures for remote sensing of wake vortices requires RHI measurements in a plane perpendicular to an aircraft's flight path, meaning that the preferred scan is in the plane perpendicular to the runway of interest. As noted previously, the radar at Logan Airport is nearly ideally located for this purpose relative to Runways 4R/22L and 4L/22R.

3.1 First Wake Vortex Measurements: 03/26/09

The first attempt to detect and measure wake vortices with the W-Band Radar occurred on March 26, 2009 during a scan sequence that began at 19:12:05 EDT for an aircraft landing on Runway 4L. Fig. 8 shows an RHI plot of the peak spectral power returns at each range gate as a function of elevation angle and peak Doppler velocity profiles for this initial detection. Fig. 9 is an extracted portion of the figure, showing a higher resolution image that includes horizontal and vertical scales at 5-m intervals; the range resolution of these measurements was 3-m; the -6 dB two-way cross track resolution was 3.1 m. The Doppler velocity portion of the figures show a classical portrayal of the two aircraft counter-rotating vortices at a horizontal distance of ~1,025-m from the radar and having a core separation of ~10-m. The vortex flow is superimposed on a background crosswind that is also evident throughout most of the RHI scan and appears to be fairly uniform at ~2-m-s⁻¹. The return power profiles of the vortices clearly show effects of centrifugal forces causing the

raindrops caught up in the vortex flow to move outward from the cores. This may be seen by the rapid transition from very low power returns of white near the centers of the vortex cores to the ambient red levels that are ~20-dB higher in relative power. At the lower central portion of the vortex pair, especially to the lower right of the left-hand vortex, there is evidence of significantly enhanced power return or radar reflectivity. This phenomenon may be due to the accumulation of larger drops being thrown out of the vortex pair in accordance with the overall flow pattern of the vortex pair in this inner flow region. Additional features of this event and other wake vortices are shown in the following sections.

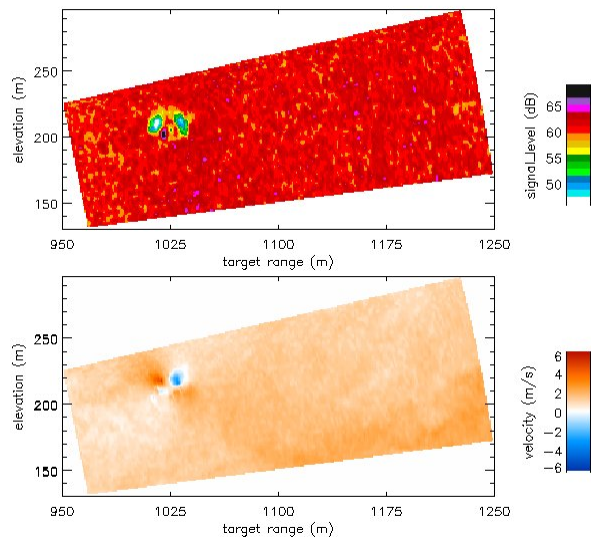


Fig. 8. First measurements of wake vortices made with the W-Band Radar on March 26, 2009 at Logan International Airport. The upper RHI is the peak spectral power level of the signal within each range bin, and the lower one is an RHI of the peak Doppler velocity.

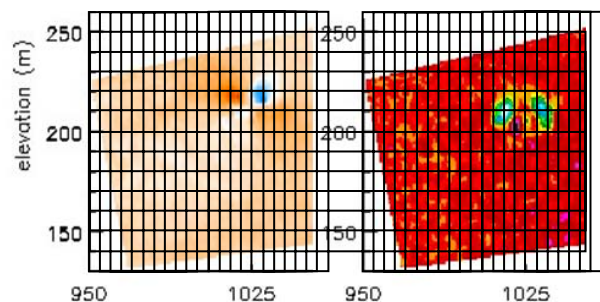


Fig. 9. The wake vortex data in Fig. 8 with higher resolution and scales overlaid at 5-m intervals on the horizontal and vertical axes.

3.1.1 Wake Vortex Transient Behavior: 03/26/09

The temporal evolution of the vortex pair presented above is illustrated in Fig. 10. The sequence is notable in that the vortices moved upwards and out of the RHI scanning region in contrast to normal behavior, which exhibits downward transport due to the mutual interaction of the two vortices. In addition, the peak power profiles show a distinct transient effect on the

atmospheric distribution of scatterers in the vicinity of the vortices, in particular, extending beneath the pair and exhibiting both enhanced and reduced peak power levels. The outside regions of the vortices have reduced peak power levels of ~10-dB from ambient levels, and the inner regions have increased levels of more than 10-dB in places. It is noted that over time these regions become more prominent by lengthening and extending downwards while the vortex pair drifts upwards and out of the RHI. Although the measurements provide clear evidence of very interesting physical phenomena, the bases for these are considered outside the scope of this paper.

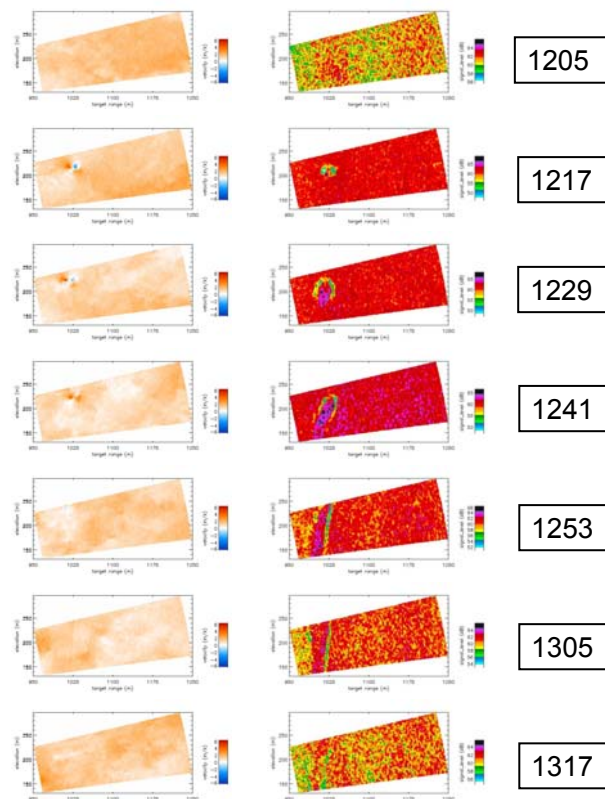


Fig. 10. Time history of the wake vortices detected by the W-Band Radar on March 26, 2009. The block numbers correspond to MMSS after 19:00 EDT.

3.1 Wake Vortex Measurements: 05/05/09

A second set of wake vortex measurements obtained on May 5, 2009 is shown in Fig. 11. In this case, the range resolution was 1.5-m and the wake was associated with an aircraft landing on Runway 4R. Since the touchdown point of this runway is much closer to the RHI plane than for Runway 4L, the initial wake detection is at a much lower height (~35-ft vs. 210-ft). The ASOS measured wind at the time was 19kts at 58°; thus, the expected crosswind speed seen by the radar should be ~5.5-m-s⁻¹. Inspection of the RHI's in Fig. 10 is seen to be consistent with this value. Unlike the previous example, these vortices were generated in a more complex atmosphere exhibiting both horizontal and vertical shear. Once formed at a height of ~32-m, the

wakes drifted downwards as expected and within ~20-s were under the influence of ground effects. The vortex separation in this case was ~25-m, compared to the previous case where the separation was ~10-m. Obviously, the wingspan of the aircraft producing the wake on May 5 had to have been much wider than the one on March 26. In addition to the Doppler velocity profiles, the peak power profiles were similar to the previous case, except for the fact that the vortex transport was downwards.

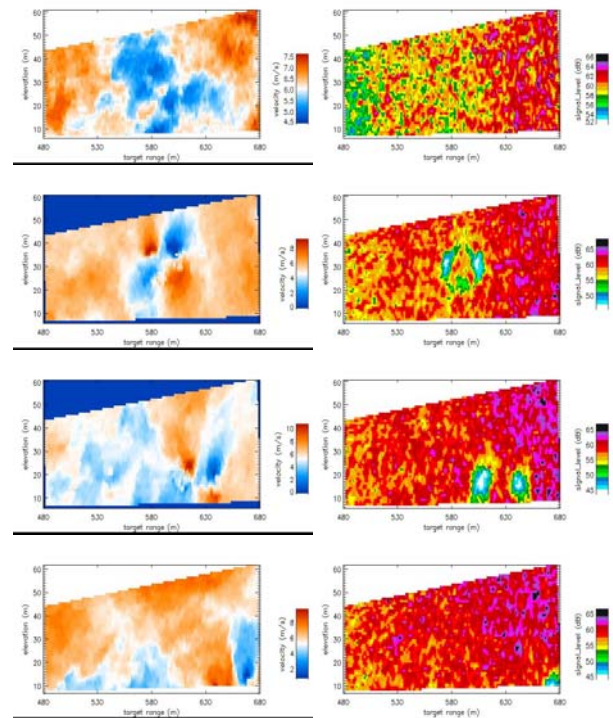


Fig. 11. Time history of wake vortices detected by the W-Band Radar on May 5, 2009. The upper pair of RHI data was taken at 10:31:47 EDT with the lower ones occurring at 8-s intervals later. Note the scale differences between the upper Doppler velocities and the other measurements.

3.1.1 Doppler Spectra: 05/05/09

In addition to the Doppler velocity and peak power RHI profiles shown in Fig. 11, Doppler velocity spectra along select ray paths at different elevation angles were processed. Examples of these for the second from the top RHI profile are given in Fig. 12. Rays above, approximately through and below the center of the vortex pair are designated as High, Mid and Low, respectively. The mean radial velocity is ~6.1-m-s⁻¹, again consistent with the previously cited ASOS value of 5.5-m-s⁻¹. As with the wind validation case discussed in Sect. 2.2, the ASOS winds would typically understate the wind speed at the height of the vortices by as much as 30%. The actual difference was 10%. The spectra demonstrate a high coherency of the measurements at each range gate and an ease for extracting quantitative

information on wake properties such as circulation intensities and core radii.

Another spectral feature of possible interest is the apparent presence of turbulence in the wake vortex volume. This is evidenced by the presence of radar signal power at velocities quite different from the dominant portion of the signal or as a large spread or variance in the spectra. A clearer picture of this turbulence is shown in Fig. 13, corresponding to the spectra of a Low Side ray that is nearer the center of the vortex pair than the Low Side ray shown in Fig 12. The enhanced turbulence is detected via the large spread in the signal near the center of the vortex pair. The exact nature of this turbulence is not dealt with in this paper.

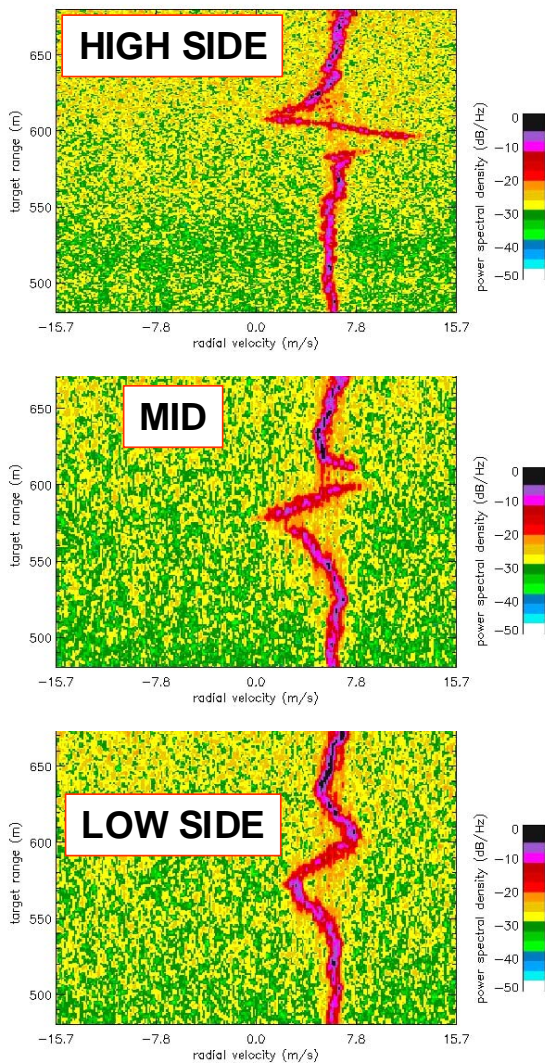


Fig. 12. Doppler velocity spectra along radar radials at different regions of the wake vortex pair shown in the second from the top profile of Fig. 11 (10:31:55 EDT). High refers to a ray above the center of the vortex pair, Mid passes approximately through the center of the pair and Low passes below the pair.

4. OTHER REMOTE SENSING TECHNIQUES

The evolution of studies on wake vortex measurements has led to a recent emphasis and reliance on LIDAR technology to investigate the properties of wakes generated by aircraft during takeoff and landing operations at airports (Hannon and Thompson, 1994; Mackey et al., 2007; Wassaf et al., 2008). Other approaches have centered on the use of microwave radar technology. Radar examples were given by Neece et al. (2005) who examined attributes of Ka-band radar, and, more recently, by Barbaresco et al. (2007) who are exploring the utility of X-band radar for wake detection and tracking. None of these system designs enable range resolutions down to 1-m as demonstrated with the W-Band Radar; the narrow beam achievable at this wavelength is also an attractive feature compared to many other radar designs. The major limiting factor of the W-Band Radar is its reliance on hydrometeor scatterers, while high power, higher wavelength systems can also respond to atmospheric refractivity gradients in the scattering volume.

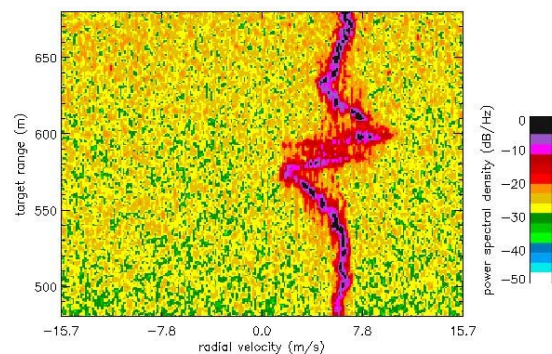


Fig. 13. Example of Doppler velocity spectra for a ray below (Low Side) the center of the vortex pair indicating considerably greater amounts of turbulence than the spectra in Fig. 12.

5. CONCLUSIONS

This paper presented the first W-Band Radar measurements of wake vortices generated by aircraft landing at an airport. The Radar was specially designed for measuring heights of ships and marine vessels in Boston Harbor in support of air traffic operations at Boston's Logan International Airport. Since its attributes closely match those desirable for detecting and tracking wake vortices, the Radar was employed in an RHI scan mode in a plane normal to parallel runways at Logan. The Radar's unique capabilities (high temporal and spatial resolution combined with appropriate short-duration scan times) were successfully applied to the detection and tracking of wake vortices in rainfall conditions.

Improvements in the radar design are clearly desirable and possible for the application. In particular, sensitivity can readily be increased by more than 20-dB, since the peak transmit power of 100-mW is much less than what is possible with kW-level klystron transmitters.

Such a system would extend the utility of the radar to greater distances to account for signal losses due to attenuation in fog and rainfall and to detection of wakes in fog.

Many other atmospheric research applications of the W-Band Radar are apparent from the data presented here and from other responses of the system under varying weather conditions. An example of the latter that is not reported here is the occurrence of short-lived severe attenuation events in dense fog that are most likely attributable to the presence of unusually high values of liquid water content along the radar's propagation path. Thus, this type of radar should prove very useful for investigations in microscale and boundary layer meteorology, atmospheric turbulence and cloud physics.

5. ACKNOWLEDGEMENTS

The results presented in this paper were made possible through support of the Massachusetts Port Authority (MASSPORT) in conjunction with the development and installation of the Tall Vessel Detection System at Logan International Airport. The wake vortex related operations of the W-Band Radar system occurred during the testing phase of the system. The encouragement of Mr. Flavio Leo, Manager of Aviation Planning at MASSPORT, is especially noteworthy.

6. REFERENCES

- Barbaresco, F., A. Jeantet and U. Meier, 2007: Wake vortex detection & monitoring by X-band Doppler radar: Paris Orly radar campaign results, IET International Conference on Radar Systems, Radar 2007, Oct. 15-18, Edinburgh, UK.
- Broderick, A. J., et al., 2008: **Wake Turbulence—An Obstacle to Increased Air Traffic Capacity**, National Research Council Committee to Conduct an Independent Assessment of the Nation's Wake Turbulence Research and Development Program, Aeronautics and Space Engineering Board, Division on Engineering and Physical Sciences (The National Academies Press, Washington, D.C.), 86pp.
- Federal Aviation Administration (FAA), 2008: Aeronautical Information Manual Official Guide to Basic Flight Information and ATC Procedures. http://www.faa.gov/air_traffic/publications/ATpubs/AIM/C hap7/aim0703.html
- Gerz, T., F. Holzäpfel and D. Darracq, 2001: Aircraft Wake Vortices – A position paper, Locate at <http://www.cerfacs.fr/~wakenet>, 43pp.
- Gerz, T, F. Holzäpfel and D. Darracq, 2002: Commercial wake vortices, Prog. in Aerospace Sciences, **38**, 181-208.
- Hallock, J. N., G. C. Greene and D. C. Burnham, 1998: Wake vortex research – A retrospective look, Air Traffic Control Quart., **6**, 161-78.
- Hannon, S. M. and J. A. Thompson, 1994: Aircraft wake vortex detection and measurement with pulsed solid-state coherent laser radar, J. Modern Optics, **41**, 2175.
- Hellmann, G., 1917: Über die Bewegung der Luft in den untersten Schichten der Atmosphäre. (2. Mitteilung.), Meteorologische Zeitschrift **34**, 273–285.
- Mackey, S. M., Y. F. Yang, H. Wassaf and M. Soares, 2007: Comparison between arrival and departure wake vortex statistics near the ground, Proc. 1st CEAS European Air and Space Conf., - Century Perspectives, Sept. 10-13, Berlin, Germany.
- Mead, J. B., I. PopStefanija, P. Kollias, B. A. Albrecht and R. Bluth, 2003: Compact airborne solid-state 95-GHz FMCW radar system, 31st AMS Conf. on Radar Meteorology, Aug. 6-8, Seattle, WA.
- Mead, J. B., T. A. Seliga and F. Leo, 2009: High resolution radar display system for height determination and display of ships in Boston Harbor, 28th Digital Avionics Systems Conference, Orlando, FL, Oct. 25-29, 2009.
- Neece, R., C. Britt, J. White, C. Nguyen, A. Mudukutore and B.I Hooper, 2005: Wake Vortex Tracking Using a 35 GHz Pulsed Doppler Radar, ICNS Conference & Workshop 2005, **May 2 – 5, 2005, Fairfax, VA.**
- Ulaby, F. T., R. K. Moore and A. K. Fung, 1981: **MICROWAVE REMOTE SENSING ACTIVE AND PASSIVE, Vol. I. Microwave Remote Sensing Fundamentals and Radiometry**, Addison-Wesley Pub. Co., Reading, MA, 456pp.
- WakeNet, 1998: WaKEEnET – Thematic Network Wake Vortex, European Commission. <http://www.cerfacs.fr/~wakenet/>
- Wassaf, H. S., A. Tabriz, F. Y. Wang and M. Soares, 2008: Atmospheric turbulence effects on near-ground wake vortex demise, 13th Conf. on Aviation Range and Aerospace Meteorology, American Meteorology Society, Jan. 20-24, New Orleans, LA.